Numerical Simulation and Comparative Assessment of PMSM Based Motor Charactersitics for Electric Vehicle Applications

[1]Virendra Swaroop Sangtani, [2]Bharat Bhushan Jain, [3] Dr. Nandkishor Gupta, [4] Guru Saran Chayal

[1]Associate Professor, Department of Electrical Engineering, Swami Keshvanand Institute of technology, Management & Gramothan, Jagatpura, Jaipur

[2]Professor, Department of Electrical Engineering, Jaipur Engineering College, Kukas, Jaipur

[3]Assistant Professor, Department of Electrical Engineering, Government Engineering College Ajmer

[4]M.Tech Student, Department of Electrical Engineering, Jaipur Engineering College, Kukas, Jaipur

virendrasangtani@rediffmail.com, drbharatjainjec@gmail.com, nkgupta1987@gmail.com, sunnyhanumangarh@gmail.com

Abstract

Worldwide, electric vehicles (EVs) are becoming more popular than traditional vehicles powered by fossil fuels. However, the higher cost of an EV's purchase means that it may remain a major roadblock for the market. Customers choose electric vehicles for a variety of reasons, including lower carbon emissions, better performance, and more. Environmental awareness and a vision for renewable energy are essential to ensuring the long-term viability of energy production. According to a recent study, the demand for electric vehicles will rise by 2-6 percent for every 1 percent increase in renewable energy sources. By altering the recharging power at a given time interval, electric vehicles (EVs) can offer new potential for delivering regulation services and a wide range of consumption options. Modeling electric vehicles is the primary subject of this dissertation. A Rinehart motion systems-AC motor controller- 'PM100DZ' will be used to replicate the performance of an Evoelectric 'AF-130' Permanent Magnet Synchronous Motor. Using this data, researchers were able to better understand how permanent-magnet motor drives work. Simscape blocks used to model PMSM and vector control are to be validated in this effort. As a last step, parameter estimation was used to tweak the Dynamic motor and Thermal models. Datasheet values and simulated data still differed, and this difference was investigated to determine its source.

Keywords:-Photovoltaic (PV), Electrical Vehicle , Characteristic Analysis, Design Simulation, Modeling

I. INTRODUCTION

Traditional fossil-fuel vehicles are losing ground to electric vehicles (EVs), which are becoming more popular around the world. But because batteries are so expensive, the price of an EV may remain the biggest obstacle to its adoption in the marketplace. Due to their zero carbon emissions and greater performance, electric vehicles have become increasingly popular with consumers. For the future of our energy supply, we need consumers who care about the environment and who have a positive outlook on renewable energy. An increase in renewable energy of just one percent is expected to bring in a 2–6 percent increase in EV demand. This chapter focuses on charging stations for electric vehicles (EVs), as well as the increasing use of distributed generators in the grid. Photovoltaic (PV) energy sources and battery storage technologies are described in detail. Lastly, the chapter wraps up by providing an overview of the proposed system's high-level design and a summary of the information in the following chapters.

As fossil fuels become increasingly scarce and greenhouse gas emissions must be reduced, a large amount of research has been done on electric vehicles (EVs) [1]. Although it has a substantial impact on EV development, the desire of consumers to switch from traditional internal combustion engine vehicles to EVs. EV demand forecasting relies heavily on the willingness of consumers to purchase electric vehicles. A key problem for electric vehicles (EVs) is the time it takes to charge. [2] Aiming to explore new methods for speeding up EV charging, this dissertation focuses on developing new techniques to reduce charging time. Fig. 1.1 shows an illustration of the three charge levels being studied and developed in the United States. [3] Electric vehicles are categorised into charging levels based on their power charging rates.

It is possible to charge EVs overnight using level I charging, which involves plugging them into a convenient power outlet (120 V) for long periods of slow charging (1.5-2.5 kW). Long driving cycles necessitate a lot of recharging, and level-I charging isn't a good fit because of its lengthy charging time. Distribution transformers, which are not allowed to rest in a large grid system with a large number of linked electric vehicles, are overburdened by long nighttime charging hours. Because Level-II charging requires a 240 V outlet, it is commonly used as the primary charging method in both private and public facilities. At this charging level, which provides power ranging from 4 - 6.6 kW over the course of three to six hours, depleted electric vehicle batteries can be recharged. The time it takes to charge at this level is the main drawback. Level II charging is further hindered by voltage sags and significant power losses in an electrical grid system with a high penetration rate of this charging technique. In order to counteract the negative consequences of level-II charge [5], control and coordination at level II are needed, but this will involve the installation of an extensive communication infrastructure. Both levels I and II require single phase power sources with onboard car chargers. Off-board chargers and three-phase power systems are used in level III fast charging (50-75 kW). By utilising fast charging stations, electric vehicles can be fully charged in under 30 minutes. Rapid EV charging stations in urban and suburban regions are also needed to alleviate range anxiety [6–7] concerns. A significant amount of stress is placed on the electrical grid while charging at high rates for level-III in a short period of time [8-9].

The electric supply sector has evolved around the main premise of centralised generating since its inception. As shown in Fig. 1.2, electrical power is supplied from enormous power plants via lengthy transmission lines and a massive distribution network to consumers in this centralised system.

A number of breakthroughs began to disrupt the fundamentals of electrical grid operating a few decades ago, resulting in the rise of DGs. Due to modern technologies and advancements in the power electronics and smart grid domains, the ambitious targets of increasing DG deployment rates into the electrical pool are possible. In addition, new legislation and policies promoting distributed generation and net metering are constantly being issued. The type of energy used to feed the deployed DG sources on the demand side, on the other hand, is a critical aspect in the DGs concept's economic feasibility in today's electrical distribution market.
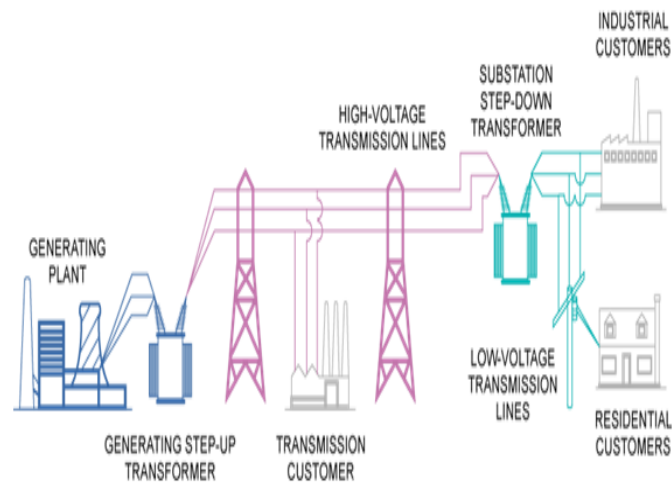
Fig. 1.1. Conventional centralized electric grid structure [12]

Solar energy is regarded as one of the most effective resources that has gained a lot of interest due to its widespread availability and long-term viability. The use of PV panels is the most popular application for solar energy. PV panels are widely used because of its unique ability to convert solar energy directly into electrical energy without the use of mechanical auxiliary equipment. PV panels can thus be used in a variety of power generation applications, ranging from low-power home uses to megawatt-scale PV power plants.

In comparison to independent PV installations, grid-connected

The ambient temperature and solar insolation levels have a significant impact on PV power generation. As a result, PV electricity has a day-to-day discontinuity as well as an intermittent character that can occur across small time intervals (minutes to hours). As a result, connecting the PV panels directly to the load without any additional systems has a negative impact on the linked electrical loads' performance.

Solar energy storage systems can help to stabilise the output power of solar energy. Energy storage devices, such as batteries, are advised to be integrated with PV sources in this research in order to maintain a constant power supply to linked loads regardless of PV source power fluctuations [13]. Furthermore, the grid integration of the hybrid PV-battery system allows for a greater degree of demand deregulation, which is a critical aspect in obtaining lower operating costs while achieving higher performance.

The objective of this research is to provide a detailed analysis of electric vehicle motor characteristics analysis of performance parameters.This project intends to model the performance of Evoelectric 'AF-130' Permanent Magnet Synchronous Motor which is controlled using a Rinehart motion systems- AC motor Controller- 'PM100DZ'.

For this research, we started with analysis of the motor and the controller which helped in providing values of various variables in modelling and simulation related to Permanent-Magnet Motor Drives. It also helped to understand the modelling of the PMSM and to validate the existing Simscape blocks for modelling PMSM and vector control.Due to time constrains the modelling of the cooling system wassimplified to a basic convective heat transfer model.The Dynamic motor model and thermal model were them fine-tuned with Parameter estimation using available experimental data. There were still some variation between the experimental and simulated data which was explored to find the cause for the

variation.

II. PROPSOED METHODOLOGY

The AF-130 electric motor is a three-phase PMSM motor that uses proprietary axial flux technology. The motor controller converts the DC power from the vehicle Energy Storage System to the 3-phase AC required by the motor. The PM100DZ uses the Vector control technology for controlling the torque output of the motor.
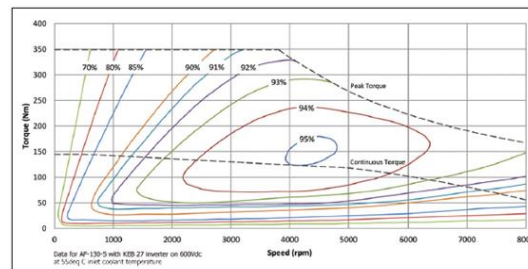

Fig 1.2 Torque-Speed Characteristics of PMSM Motor

Table 1.1 (Description of Protection Scheme- Vehicle)

Parameters	Specifications
Short Circuit Protection	Yes
Hardware Over-current Protection	Yes
Vehicle System Power	9.. 16VDC (12V Systems)
Operating Temperature Range – coolant water – no derating	-40 +80ºC
Isolation – High-Voltage to Low-Voltage	1000Vrms
Isolation – High-Voltage to Case	1000Vrms
Isolation – Low-Voltage to Case	50V
Operating Temperature Range – coolant water – derated output power	-40.. +105ºC
Non-Operating Temperature	-40 .. +115ºC
Storage Temperature	-55 .. +105ºC
Coolant Type	50/50 EGW
Coolant Flow Rate	8 – 12 LPM
Coolant Pressure Drop	0.2 bar for PM100xx
Maximum Coolant Pressure (above ambient)	1.4 bar
Operating Shock (ISO 16750-3, Test 4.2.2.2)	500 m/s2 (50g)
Operating Vibration (ISO 16750-3, 4.1.2.4 Test IV)	27.8 m/s2 (3grms)
Environmental Protection Class	IP6K9K

Table 1.2 (Specifications of Motor Used in Proposed Simulation)

Parameters	Specifications
Type	PM Synchronous -Axial Flux
Maximum Speed	8000 rpm
Nominal Torque	145 Nm
Peak Torque (for up to 60s)	250Nm
Peak Torque (for up to 20s)	350Nm
Nominal Output Power	121.47 kW
Peak Output Power (for up to 60s)	209.43 kW
Peak Output Power (for up to 20s)	293.21 kW
Torque Density	11.5Nm/kg
Power Density	4.6kW/kg
Peak Efficiency	95.10%
Coolant Medium	Water/Glycol (50/50)
Coolant Flow Rate	> 8l/min
Dimensions	110 mm (L) x 300 mm (D)at 30.5 kg

The PMSM and SM both have similar stator and wound rotor respectively, the induced currents in the rotor of PMSM are negligible and both produce similar back EMF. Hence the mathematical model of a PMSM is similar to that of the wound rotor. Therefore, the d-q equations of the PMSM are:

$$v_q = Ri_q + p\lambda_q + \omega_s\lambda_d \quad (1.1)$$
$$v_d = Ri_d + p\lambda_d + \omega_s\lambda_q \quad (1.2)$$

Where,

$$\lambda_q = L_q i_q$$
$$\lambda_d = L_d i_d + \lambda_{af}$$

v_d and v_q are q and d axis voltage, i_q and i_d are q and d axis stator current, i_d and i_q are the d, q axis stator currents, L_d and L_q, are the d, q axis inductances, λ_d and λ_q, are the d, q axis stator flux linkages, while R and ω_s, are the stator resistance and inverter frequency, respectively. λ_{af} is the flux linkage due to the rotor magnets linking the stator. The electric torque is

$$T_e = \frac{3P[\lambda_{af}i_q + (L_d - L_q)i_d i_q]}{2} \quad (1.3)$$

And the equation of motor dynamics is

$$T_e = T_L + B\omega_r + Jp\omega_r \quad (1.4)$$

P is the number of pole pairs, T_L is the load torque, B is the damping coefficient, ω_r, is the rotor speed, and J is the moment of inertia.

Simscape comes with a general model of the PMSM machines here are a few details about the Simscape PMSM block:

The Permanent Magnet Synchronous Machine block operates in either generator or motor mode. The mode of operation is dictated by the sign of the mechanical torque (positive for motor mode, negative for generator mode).

The block has the options to opt for either sinusoidal or Trapezoidal flux since Pragasen Pillay and Ramu Krishnan have assumed a sinusoidal flux we will be going with that option. The equations driving this block are:

$$\frac{d}{dt}i_d = \frac{1}{L_d}v_d - \frac{R}{L_d}i_d + \frac{L_q}{L_d}p\omega_m i_q \quad (1.5)$$

$$\frac{d}{dt}i_q = \frac{1}{L_q}v_q - \frac{R}{L_q}i_q + \frac{L_d}{L_q}p\omega_m i_d - \frac{\lambda p\omega_m}{L_q} \qquad (1.6)$$

$$\text{Te} = 1.5p[\lambda iq + (Ld - Lq)idiq] \qquad (1.7)$$

Here, L_q, L_d are q and d axis inductances, R is Resistance of the stator windings. i_q, i_d are q and d axis currents. v_q, v_d are q and d axis voltages. ω_m is Angular velocity of the rotor. λ is Amplitude of the flux induced by the permanent magnets of the rotor in the stator phases. p is Number of pole pairs and T_e is Electromagnetic torque

And the dynamic motor equation

$$\frac{d}{dt}\omega_r = \frac{1}{J}(T_e - T_f - F\omega_m - T_m) \qquad (1.8)$$

$$\frac{d}{dt}\theta = \omega_m \qquad (1.9)$$

Where J is combined Inertia and rotor load, F is viscous friction, θ is rotor angle position ω_m is Angular velocity of the rotor, T_m is shaft mechanical torque and T_f is shaft static friction Torque.

Comparing the two models we can see that the core concept behind the model in the research paper and the model in the simscape is same although the assumption in the paper referred are more and hence we conclude we can use the PMSM block and we can use a simplier version by neglecting some variables.

Vector control is normally used in ac machines to convert them, performance wise, into equivalent separately excited dc machines which have highly desirable control characteristics. Analysis of literature explains vector control as "a variable-frequency drive (VFD) control method in which the stator currents of a three-phase AC electric motor are identified as two orthogonal components that can be visualized with a vector. One component defines the magnetic flux of the motor, the other the torque. The control system of the drive calculates the corresponding current component references from the flux and torque references given by the drive's speed control. The rotor flux linkage revolves at rotor speed ωr and is positioned away from a stationary reference by the rotor angular position, given by
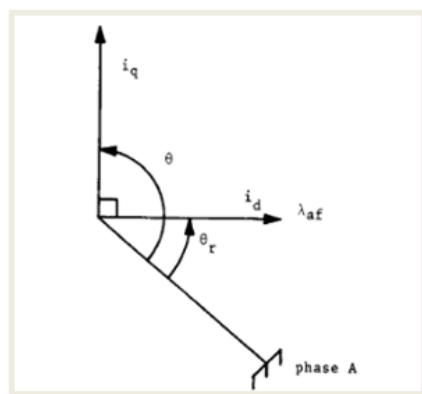

Fig 1.3 Phase Diagram of Vector Control

$\theta_r = \int \omega_r dt$ (1.10)

where t is the time. If id is forced to be zero, then

$\lambda_d = \lambda_{af}$ (1.11)

$T_e = \frac{3P\lambda_{af}}{2}$ (1.12)

Since the magnetic flux is a constant, the torque is directly proportinal to the q axis current. This is represented as

$T_e = K_t i_q$ (1.13)

Where

$Kt = \frac{3P\lambda_{af}}{2}$ (1.14)

Torque equation is similar to that of a seperately excited DC motor.Simscape has a vector control PMSM block which is shown below
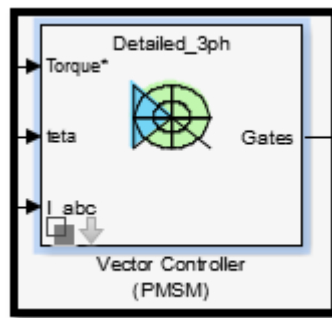
Fig 1.4 Design of Vector Control of PMSM
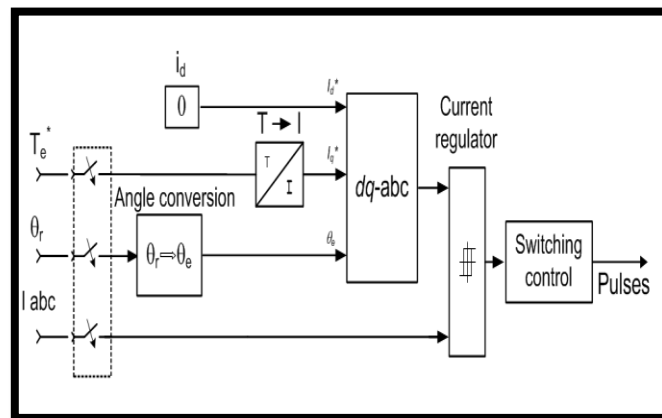
Fig 1.5 Subsystem Design of Vector Control of PMSM

This block uses the vector control logic for PMSM and we will be using this to model our complete dynamics. The heat generated is determined by the difference between the electric power from Battery and the mechanical power generated hence this heat accounts for heat generated in MCU and motor both. The cooling model has been simplified because of time constrain and because of having an already complex motor model. The figure below shows a conceptual image of logic. This logic is implemented using simple convective heat transfer block where heat exchange is taking place

III.RESULTS

This section discuss step by step simulation process which have been followed in the design and development of controlled strategies of the designed electric vehicle drive. The simulation has been done to implement complete working Simulink model of PMSM system along with vector control and heat management system to enable the understanding of performance analysis and improvement methods.Since many variable for modeling the motor are unknown we will create single value variables for those parameters so that we can utilize them for parameters estimation. A step by step modeling guide is not needed as most of the blocks are present in Simscape understanding the functionality and parameter estimation is given focus.Subsystem Soft ECU receives the signals from HCU and sensors and calculates the desired action to get the required torque. This subsystem is imported from the provided SOFT MCU model because the provided model in sufficient for our requirements.
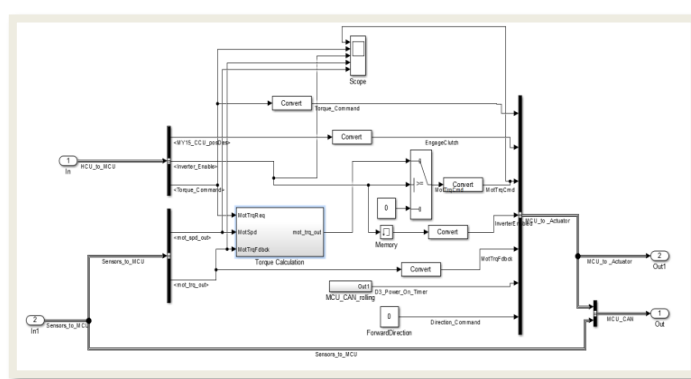

Fig 1.6 Simulink Model of Mechanical Characteristic Analysis

This block uses the vector control logic for PMSM and we will be using this to model our complete dynamics. The heat generated is determined by the difference between the electric power from Battery and the mechanical power generated hence this heat accounts for heat generated in MCU and motor both.
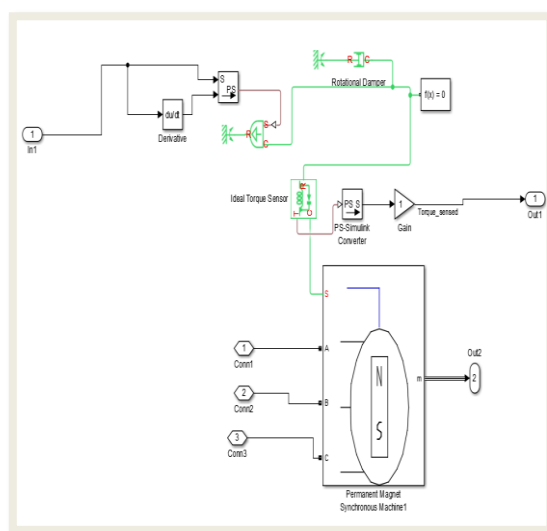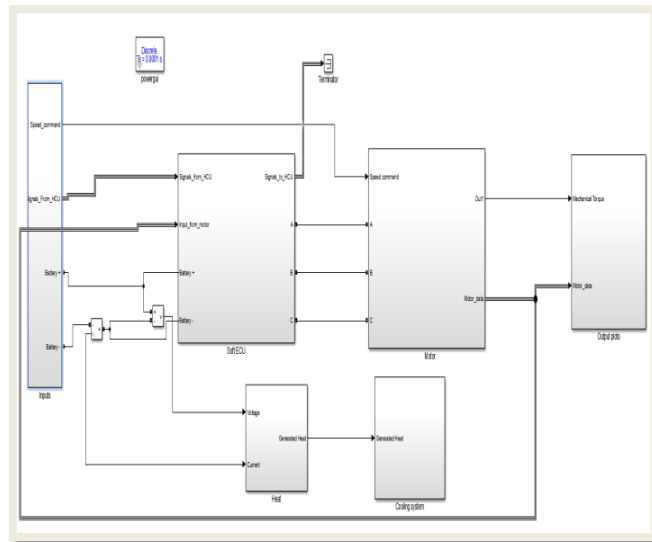

Fig 1.7 Motor Control System

Fig 1.8 Simulink Model of Complete System

The cooling model has been simplified because of time constrain and because of having an already complex motor model. The figure below shows a conceptual image of logic. This logic is implemented using simple convective heat transfer block where heat exchange is taking place.

The pressure drop and the flow rate is provided in the motor specification this can be further altered to get desired cooling performance. The control of cooling and pumps is handled by HCU.
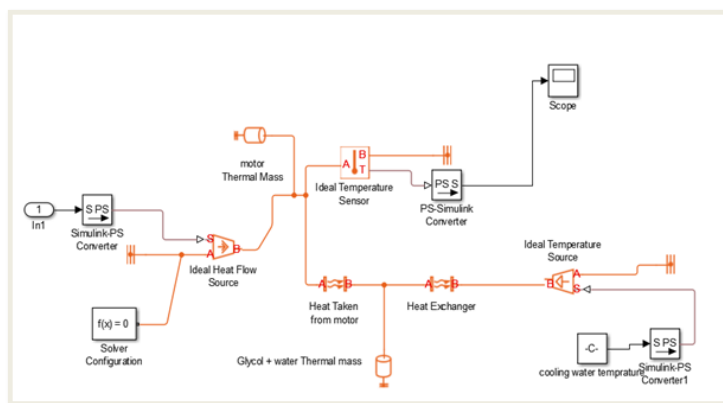

Fig 1.9 Design of Cooling Subsystem

The design of measurement system has been done to analyze the performance of the simulated system under operational condition. The system has been simulated to obtain electrical, mechanical and thermal parameters of the designed vehicle system under operational condition.
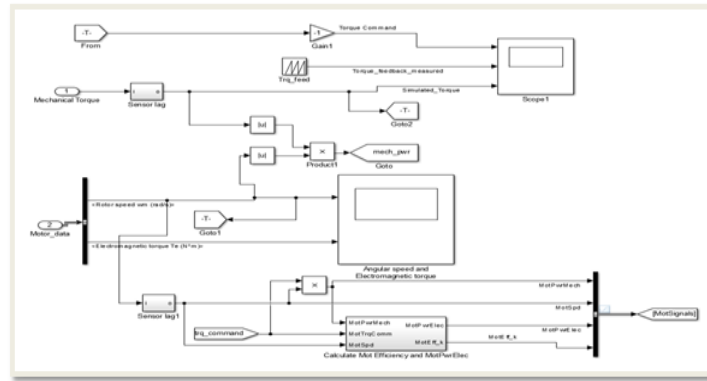
Fig 1.10   Design of Measurement System

Initialize the following variables with values somewhere around the values provided. These provided values are final values obtained after parameter estimation.

Table 5.1 Important Simulation Parameters

Parameters	Value	Parameters	Value
Ts	1.00E-05	resistance	0.11607
Stator_phase_resistance	0.0490392	fluxByMagnet	0.17491
Armature_inductance	6.32E-04	temp_amb	300
flux_linkage	0.17216	coolant_cp	200.07
Pole_pairs	3	coolant_mass	2.2147
induced_flux	0.17197	hac	9.2743
currenthysteresisband	0.1	hcm	35.286
Snubberresisrance	1.00E+04	htArea	0.2
Ron	7.83E-06	motor_cp	12.5
Inrt	2.50E-04	radiator_area	2.3951
Damp	4.18E-04	motor_mass	30
battery_Voltage	390.4254		

The parameter estimation was done separately for motor dynamics and thermal to improve performance. Due to low Simulation speed it was very difficult to simulate the test for whole 1288 secs therefore, for testing and simulation a 76 sec of data clip was taken from the test data and then the result was obtained.
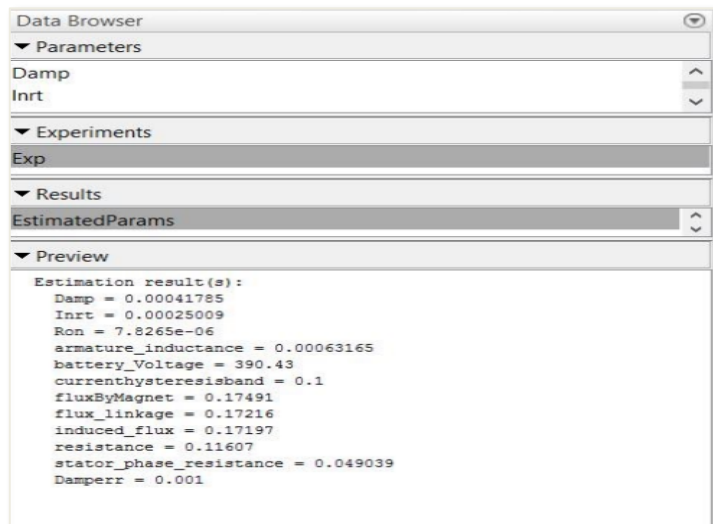
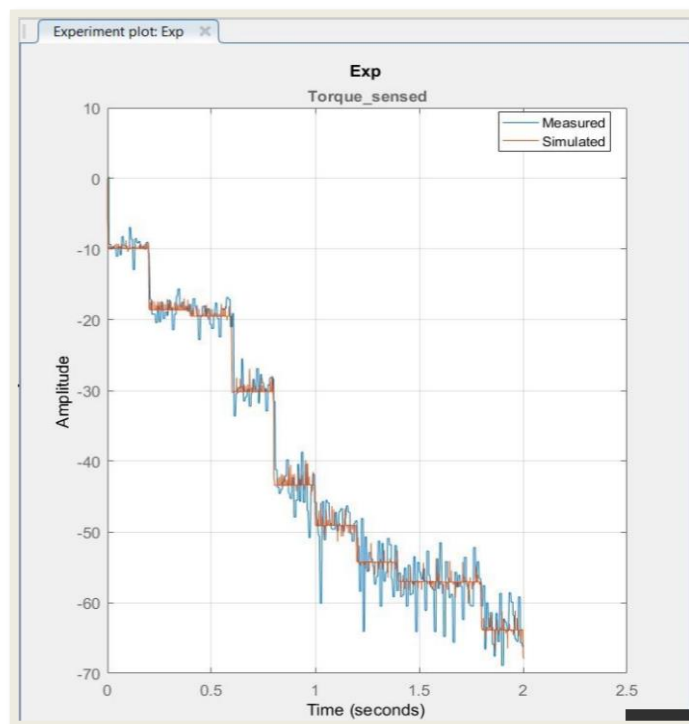Fig 5.11   Electrical Parameter Estimation

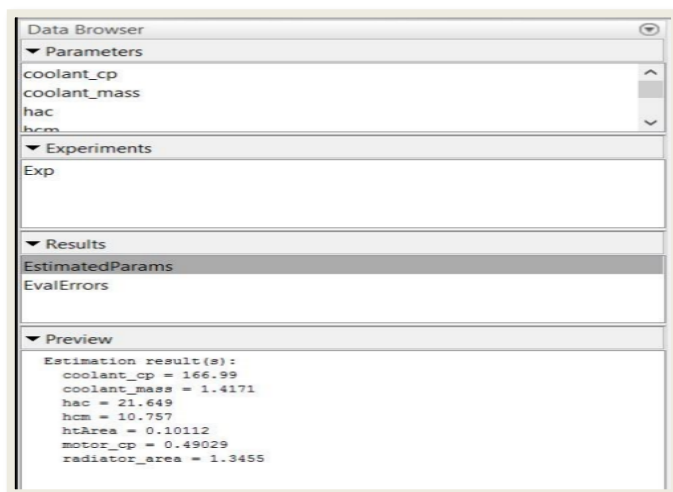Fig 1.12   Mechanical Model Parameter Estimation

Fig 1.13   Thermal Model Parameter Estimation
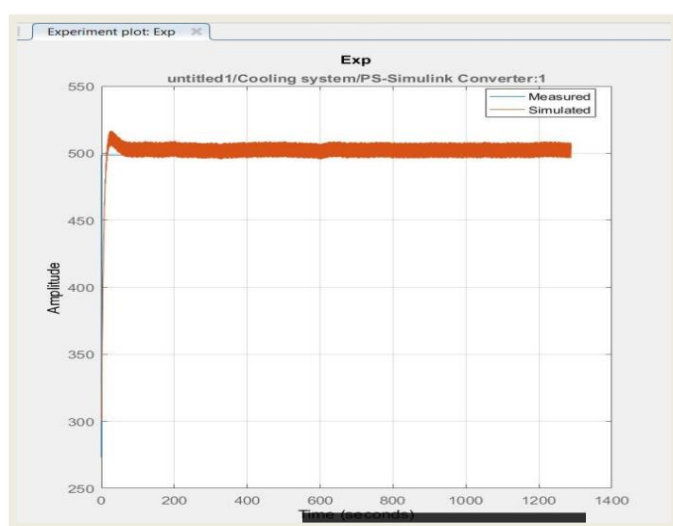

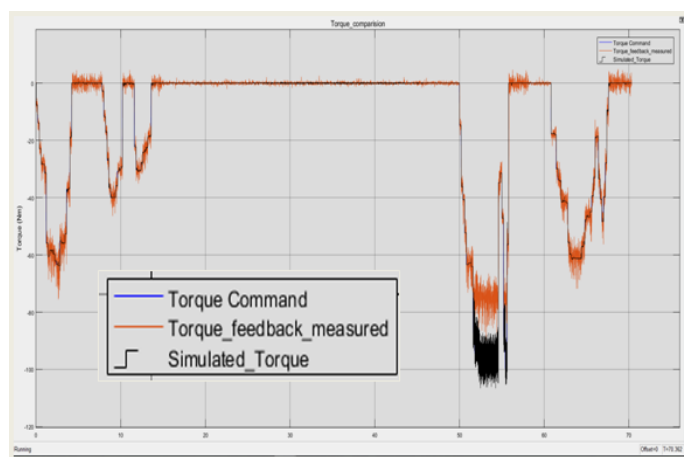Fig 1.14   Cooling Analysis

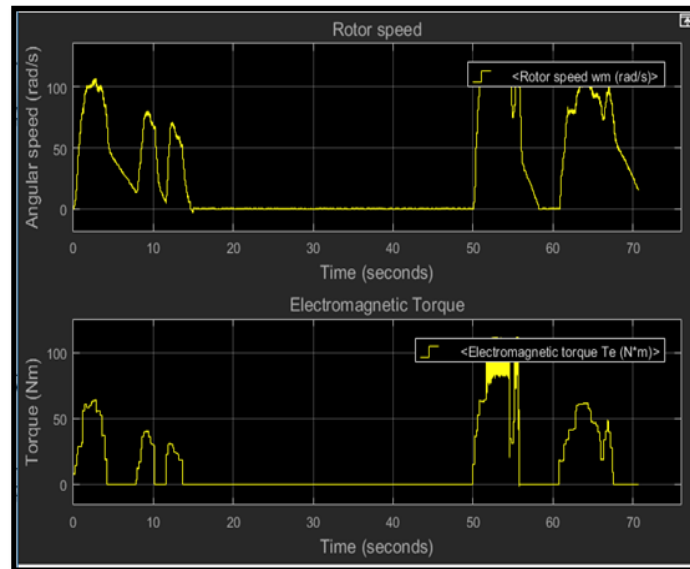Fig 1.15   Torque Analysis of Proposed System

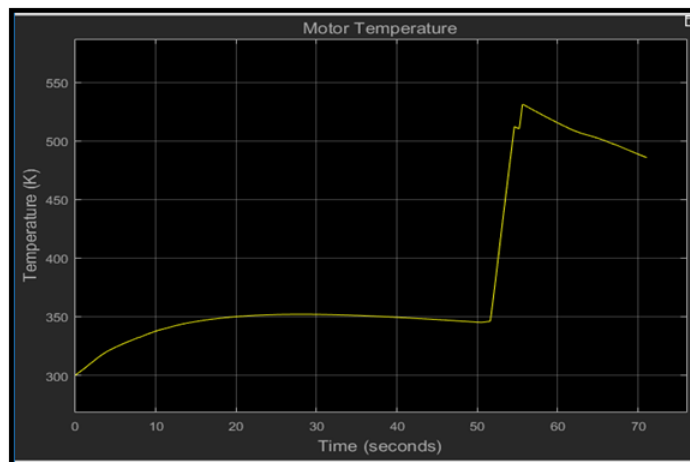Fig 1.16   Rotor Speed and Electromagnetic Torque

Fig 1.17 Temperature Analysis

When the initial torque command is fired, the motor is unable to meet the torque demand and just provides 20% of the torque demand. There are two possibilities for this. One, a mistake in setup but it seems unlikely as the later torque demand is successfully met, another possible reason for this could be that "Damper windings were used to run the machine up to speed on induction motor action with the machine pulling into synchronism by a combination of the reluctance and synchronous motor torques provided by the magnet. During the startup, the magnet exerts a braking torque that opposes the induction-motor-type torque provided by the damper windings.Second abnormality in the data obtained from datasheet and simulation is the temperature measure at motor the value remains at 0^0C for few mili- seconds and then jumps to 225.60C. The initial values might be due to the response time of the sensor which means that the system was always at 225.6^{0}C. The flow of heat occurs due to the difference in temperature of the two bodies first. The motor remaining at 225.6^{0}C throughout experiment that means there is a perfect sync between the coolant flow rate and torque demand and hence all heat produced is taken by the coolant instantaneously. Which seems

highly unlikely which forces the conclusion that there is some mistake in the recorded data although a we have developed a cooling system which keeps the motor within safe operating temperature range this model can be modified to fit true data when available.Otherwise model is very close to the actual performance of the motor and is ready to be used as a part of more complex systems.Although model runs slow the simulation speed can be increased by increasing the step size (Ts) in MATLAB to suit the requirements although the accuracy would deteriorate with increasing step size. Ts = 1e-5 gives the best results, but the model is set to Ts = 1e-4 for better speed.This explains the proposed simulation for analysis of several characteristics and figure of merits of the motor and the parametric evaluation with the datasheet for the validation of simulation as well as analysis of errors. The proposed simulation is useful for design and modeling of electric vehicle and to understand accurate mathematical model of the motors and subsidiary elements of the electric vehicle.

VII.CONCLUSION

IThe motor is unable to match the torque demand when the initial torque instruction is issued, and only offers 20% of the torque need. This could be one of two things. One possibility is that "Damper windings were used to run the machine up to speed on induction motor action, with the machine pulling into synchronism by a combination of the reluctance and synchronous motor torques provided by the magnet." Another possibility is that "Damper windings were used to run the machine up to speed on induction motor action, with the machine pulling into synchronism by a combination of the reluctance and synchronous motor torques provided by the magnet during startup, the magnet produces a braking torque that resists the damper windings' induction-motor-type torque.The second anomaly in the datasheet is the temperature measurement at the motor, which lingers at 0^0C for a few milliseconds before jumping to 225.6^0C.Although we have devised a cooling mechanism that keeps the motor within a safe operating temperature range, this model can be adjusted to reflect genuine data when available, which seems exceedingly unlikely. Otherwise, the model is quite close to the motor's actual performance and is ready to be employed in more complicated systemsv.

REFERENCES

[1] Badea, Gheorghe, Raluca-Andreea Felseghi, Mihai Varlam, Constantin Filote, Mihai Culcer, Mariana Iliescu, and Maria Simona Răboacă. "Design and simulation of romanian solar energy charging station for electric vehicles." Energies 12, no. 1, 2019.

[2] Mouli, G.C., Bauer, P. and Zeman, M., "System design for a solar powered electric vehicle charging station for workplaces", Applied Energy, 168, pp.434-443, 2016.

[3] Vignesh, T. R., M. Swathisriranjani, R. Sundar, S. Saravanan, and T. Thenmozhi. "Controller for Charging Electric Vehicles Using Solar Energy." Journal of Engineering Research and Application 10, no. 01, pp. 49-53, 2020.

[4] Vanitha, D. D. . (2022). Comparative Analysis of Power switches MOFET and IGBT Used in Power Applications. International Journal on Recent Technologies in Mechanical and Electrical Engineering, 9(5), 01–09. https://doi.org/10.17762/ijrmee.v9i5.368

[5]   Suganthi, D., and K. Jamuna. "Charging and Discharging Characterization of a Community Electric Vehicle Batteries." In Emerging Solutions for e-Mobility and Smart Grids, pp. 213-223. Springer, Singapore, 2021.

[6]   Harika, S., R. Seyezhai, and A. Jawahar. "Investigation of DC Fast Charging Topologies for Electric Vehicle Charging Station (EVCS)." In TENCON 2019-2019 IEEE Region 10 Conference (TENCON), pp. 1148-1153. IEEE, 2019.

[7]   Gautham Ram Chandra Mouli, Pavol Bauer and Miro Zeman, "System design for a solar powered electric vehicle charging station for workplaces." Applied Energy, 2016.

[8]   Ravikant, U. Chauhan, V. Singh, A. Rani and S. Bade, "PV Fed Sliding Mode controlled SEPIC converter with Single Phase Inverter," 2020 5th International Conference on Communication and Electronics Systems (ICCES), pp. 20-25, 2020.

[9]   Xu, Tong, Hengshu Zhu, Xiangyu Zhao, Qi Liu, Hao Zhong, Enhong Chen, and Hui Xiong. "Taxi driving behavior analysis in latent vehicle-to-vehicle networks: A social influence perspective." In Proceedings of the 22nd ACM SIGKDD International Conference on Knowledge Discovery and Data Mining, pp. 1285-1294. 2016.

[10]   Philip, A. M., and D. S. . Hemalatha. "Identifying Arrhythmias Based on ECG Classification Using Enhanced-PCA and Enhanced-SVM Methods". International Journal on Recent and Innovation Trends in Computing and Communication, vol. 10, no. 5, May 2022, pp. 01-12, doi:10.17762/ijritcc.v10i5.5542.

[11]   Anjali, Raj Kumar Kaushik and Deepak Sharma, "Analyzing the Effect of Partial Shading on Performance of Grid Connected Solar PV System," 2018 3rd International Conference and Workshops on Recent Advances and Innovations in Engineering (ICRAIE), 2018, pp. 1-4, doi: 10.1109/ICRAIE.2018.8710395.

[12]   Rajkumar Kaushik, Om Prakash Mahela, Pramod Kumar Bhatt, Baseem Khan, Sanjeevikumar Padmanaban and Frede Blaabjerg "A Hybrid Algorithm for Recognition of Power Quality Disturbances," in IEEE Access, vol. 8, pp. 229184-229200, 2020, doi: 10.1109/ACCESS.2020.3046425.

[13]   Hoda, S. A. ., and D. A. C. . Mondal. "A Study of Data Security on E-Governance Using Steganographic Optimization Algorithms". International Journal on Recent and Innovation Trends in Computing and Communication, vol. 10, no. 5, May 2022, pp. 13-21, doi:10.17762/ijritcc.v10i5.5548.

[14]   Rajkumar Kaushik, Om Prakash Mahela, Pramod Kumar Bhatt, Baseem Khan, Akhil Ranjan Garg, Hassan Haes Alhelou and Pierluigi Siano "Recognition of Islanding and Operational Events in Power System With Renewable Energy Penetration Using a Stockwell Transform-Based Method," in IEEE Systems Journal, doi: 10.1109/JSYST.2020.3020919.

[15]   Rajkumar Kaushik, Om Prakash Mahela, Pramod Kumar Bhatt, "Hybrid Algorithm for Detection of Events and Power Quality Disturbances Associated with Distribution Network in the Presence of Wind Energy," 2021 International Conference on Advance Computing and Innovative Technologies in Engineering (ICACITE), 2021, pp. 415-420, doi: 10.1109/ICACITE51222.2021.9404665.

[16]   Kaushik RK, Pragati. Analysis and Case Study of Power Transmission and Distribution. J Adv Res Power Electro Power Sys 2020; 7(2):1-3.

[17] R. Kaushik, O. P. Mahela and P. K. Bhatt, "Events Recognition and Power Quality Estimation in Distribution Network in the Presence of Solar PV Generation," 2021 10th IEEE International Conference on Communication Systems and Network Technologies (CSNT), 2021, pp. 305-311, doi: 10.1109/CSNT51715.2021.9509681.

[18] D. B. B. J. H. U. Rajkumar Kaushik, "Identification and Classification of Symmetrical and Unsymmetrical Faults using Stockwell Transform", DE, pp. 8600- 8609, Aug. 2021.

[19] N. A. Farooqui, A. K. Mishra, and R. Mehra, "IOT based Automated Greenhouse Using Machine Learning Approach", Int J Intell Syst Appl Eng, vol. 10, no. 2, pp. 226–231, May 2022.

[20] Simiran Kuwera, Sunil Agarwal, Rajkumar Kaushik, "Application of Optimization Techniques for Optimal Capacitor Placement and Sizing in Distribution System: A Review" International Journal of Engineering Trends and Applications (IJETA) – Volume 8, Issue 5, Sep-Oct 2021.

[21] Rajkumar Kaushik, Akash Rawat, Arpita Tiwari, "An Overview on Robotics and Control Systems" International Journal of Technical Research & Science (IJTRS), Volume 6, Issue 10, pg. 13-17, October 2021.

[22] Akash Rawat, Rajkumar Kaushik, Arpita Tiwari, "An Overview of MIMOOFDM System for Wireless Communication" International Journal of Technical Research & Science (IJTRS), Volume 6, Issue 10, pg. 01-04, October 2021.

[23] Vijay, Aditi, Ashutosh Gupta, Ashwani Pal, B. Sriswathi, Geetika Mathur, and Satish Kumar Alaria. "IoT SOCIAL DISTANCING & MONITORING ROBOT FOR QUEUE." *International Journal of Engineering Trends and Applications* 8.

[24] Mishra, Pratiksha, Satish Kumar Alaria, and Prakash Dangi. 2021. "Design and Comparison of LEACH and Improved Centralized LEACH in Wireless Sensor Network". *International Journal on Recent and Innovation Trends in Computing and Communication* 9 (5):34-39. https://doi.org/10.17762/ijritcc.v9i5.5478.

[25] Kumar, Surendra, Satish Alaria, and Vijay Kumar. "Prevention in sleep deprivation attack in MANET." *International Journal of Latest Technology in Engineering (IJLTEMAS)* 4, no. 2 (2015): 139-144.

[26] J. . Hermina, N. S. . Karpagam, P. . Deepika, D. S. . Jeslet, and D. Komarasamy, "A Novel Approach to Detect Social Distancing Among People in College Campus", Int J Intell Syst Appl Eng, vol. 10, no. 2, pp. 153–158, May 2022.

[27] Satish Kumar Alaria, S.R. Dogiwal. 2013. "Reducing the Packets Loss Using New MAC Protocol". *International Journal on Recent and Innovation Trends in Computing and Communication* 1 (9):747-51. https://doi.org/10.17762/ijritcc.v1i9.2856.

[28] A. Chawla, "Phishing website analysis and detection using Machine Learning", Int J Intell Syst Appl Eng, vol. 10, no. 1, pp. 10–16, Mar. 2022.